Published in final edited form as:
Nature. 2017 May 18; 545(7654): 350–354. doi:10.1038/nature22331.

Floor plate-derived netrin-1 is dispensable for commissural axon guidance

Chloé Dominici[#1], **Juan Antonio Moreno-Bravo**[#1], **Sergi Roig Puiggros**[1,2], **Quentin Rappeneau**[1], **Nicolas Rama**[2], **Pauline Vieugue**[2], **Agnes Bernet**[2], **Patrick Mehlen**[2,*], and **Alain Chédotal**[1,*]

[1]Sorbonne Universités, UPMC Univ Paris 06, INSERM, CNRS, Institut de la Vision, 17 Rue Moreau, 75012 Paris, France

[2]Apoptosis, Cancer and Development Laboratory, Equipe labellisée 'La Ligue', LabEx DEVweCAN, Centre de Recherche en Cancérologie de Lyon, INSERM U1052-CNRS UMR5286, Université de Lyon, Centre Léon Bérard, 69008 Lyon, France

[#] These authors contributed equally to this work.

Abstract

Netrin-1 is an evolutionarily conserved secreted extracellular matrix protein discovered using genetic and biochemical screens for its role in axon guidance at the central nervous system (CNS) midline1,2. Netrin-1 is expressed by cells localized at CNS midline, such as the floor plate in vertebrate embryos1,3. Growth cone turning assays and 3D gel diffusion assays showed that netrin-1 can attract commissural axons2,4–6. Loss-of-function experiments further demonstrated that commissural axon extension to the midline is severely impaired in absence of netrin-13,7–9. Together these data support a model in which commissural axons are attracted by a netrin-1 gradient diffusing from the midline. Here, we selectively ablated netrin-1 expression in floor plate cells using a *Netrin-1* conditional mouse line. We found that hindbrain and spinal cord commissural axons develop normally in absence of floor plate-derived netrin-1. Furthermore, we show that netrin-1 is highly expressed by cells in the ventricular zone with the potential to release it at the pial surface where it binds to commissural axons. Importantly, netrin-1 deletion from the ventricular zone phenocopies commissural axon guidance defects previously described in *Netrin-1* knockout mice. These results show that the classical textbook view that attraction of commissural axons is mediated by a gradient of floor plate-derived netrin-1 is inaccurate and that netrin-1 primarily acts locally by promoting growth cone adhesion.

[*]Correspondence and requests for materials should be addressed to A.C alain.chedotal@inserm.fr, patrick.mehlen@lyon.unicancer.fr.

Authors contributions

AC, AB and PM, designed the experiments. CD, JAMB, NR, PV, QR and SRP performed the experiments. AC, CD and JAMB prepared the figures. AC and PM supervised the project and wrote the manuscript.

Authors information

Reprints and permissions information is available at www.nature.com/reprints.

The authors declare no competing interest.

Data availability statement

The data that support the findings of this study are available from the corresponding author upon reasonable request.

Europe PMC Funders Author Manuscripts

Mouse commissural neurons are diverse and comprise many subtypes10. In the midbrain, hindbrain and spinal cord, commissural neurons transiently express the Robo3 receptor 11,12 (Fig. 1a). At embryonic day 9.5 (E9.5), the first commissural neurons cross the floor plate13 where netrin-1 expression is the highest 4,7,14. As previously shown, *netrin-1* mRNA is also expressed in neural progenitors of the basal plate ventricular zone (VZ) (Fig. 1b, Fig. 2, Extended Data Figs 1 and 2). Netrin-1 protein is in the floor plate (labeled with Alcam/BEN a floor plate marker12) and along commissural axons (Fig. 1c, Extended Data Figs 1 and 2). The netrin-1 antibody, did not cross-react with netrin-3 (Extended Data Fig. 1d).

Is dorsal netrin-1 produced locally in the VZ or does it diffuse from the FP? We detected netrin-1 on the radial processes and basal endfeet of VZ neural progenitors which are bipolar cells extending from the ventricular surface to the pia (Fig. 1, Extended Data Fig. 1). We confirmed the presence of netrin-1 in VZ precursors using *Netrin-1* hypomorphs (*Netrin-1*^{ßgeo}) in which netrin-1 is fused to ß-galactosidase (ß-gal) and trapped into endosomes (Fig. 1d)7. In *Netrin-1*$^{ßgeo/+}$ embryos, netrin-1+/ß-gal+ puncta are in the floor plate and VZ but not in commissural neurons. However, commissural axons were netrin-1-immunoreactive (due to the wild type allele; Fig. 1d and Extended Data Fig. 1c). The specificity of the netrin-1 axonal-immunolabeling is supported by its absence in *Netrin-1*$^{ßgeo/ßgeo}$ embryos (Fig. 1e). A ventricular source of netrin-1 was confirmed with nestin, a marker of neural progenitors. At E10.5-E13, neural progenitor processes extending to the pial surface coexpressed netrin-1 and nestin (Fig. 1f and Extended Data Fig. 1g and Fig. 4h). This suggests that in the dorsal hindbrain and spinal cord, netrin-1 originates from VZ precursors rather than floor plate.

Which source of netrin-1 do pioneer commissural axons encounter at the onset of their extension? At E9-E9.5, the first Robo3+ commissural growth cones appear in the marginal layer of the hindbrain containing high-levels of netrin-1 (Fig. 1g). This was confirmed using a *Ptf1a:Cre*^{ERT2}*;Rosa*^{Tom} reporter line15 (Fig. 1h). Ptfa1 is expressed by diverse hindbrain commissural neuron progenitors, including those of the inferior olivary nucleus16 (ION; see below). Importantly, commissural axon guidance errors were observed in *Netrin-1*$^{ßgeo/ßgeo}$ hypomorphs embryos as soon as growth cones appear (Fig. 1i). These results suggest that netrin-1 is released or transported locally by neural progenitors to the pial surface and guides pioneer commissural axons by promoting their initial extension at the CNS periphery in the first leg of their trek. Netrin-1 accumulation on commissural axons might create a permissive pathway for follower axons.

The role of floor-plate-derived *netrin-1* in mouse commissural axon guidance *in vivo* is supported by the phenotypic analysis of *Netrin-1* hypomorphs7 and *Netrin-1* null embryos8,9. To identify the critical source of netrin-1 for mediating commissural axon guidance, we crossed a novel netrin-1 conditional mouse line (*Netrin-1*$^{L/L}$) to three mouse lines expressing Cre recombinase: (1) ubiquitously, (2) only in the floor plate, or (3) in all the neural tube except the floor plate. In homozygous (*Netrin-1*$^{Δ/Δ}$) null embryos, in which netrin-1 was ubiquitously deleted, no *netrin-1* mRNA is detectable in the hindbrain and spinal cord (Fig. 1j and not shown), in contrast to a residual expression in *Netrin-1*$^{ßgeo/ßgeo}$

hypomorphs (Extended Data Fig. 2a-c). Likewise, netrin-1 immunolabeling is abrogated in E11-E13 *Netrin-1*$^{\Delta/\Delta}$ embryos (Fig. 1j, Extended Data Fig. 1h,i). Netrin-1 immunoreactivity persisted on commissural axons in absence of permeabilization suggesting that some netrin-1 is at their extracellular surface (Extended Data Fig. 1j). This suggests that commissural axons and precursors could accumulate or internalize netrin-1, possibly in a Dcc-dependent manner as shown in *Drosophila* 17. Accordingly, Dcc is not only expressed by E11 and E13 commissural axons, but also by neural progenitors in the hindbrain (Fig. 1k). The specificity of the Dcc antibody was demonstrated by the lack of staining in *Dcc* knockout embryos18 (Extended Data Fig. 1k). In the E13 cerebellar plate (Fig. 1l), 3-hour pulse labeling with EdU (5-ethynyl-2'-deoxyuridine) and immunostaining for the stem cell marker Sox2 confirmed that Dcc expression by neural progenitors (Fig. 1m). Radial progenitor processes extended normally in *Netrin-1*$^{\Delta/\Delta}$ embryos (Extended Data Fig. 1l).

Next, we analyzed the consequences from floor plate-specific deletion of netrin-1 on commissural axon development (Figs 2 and 3). As performed previously19, we used a line expressing Cre recombinase fused to green fluorescent protein (GFP) under the control of the sonic hedgehog (Shh) promoter. Crossing *Shh:Cre* with *Rosa*^{Tom} line showed that Cre was active in E9 floor plate, before commissural axons reach it (Fig. 2a, d). Neither Tomato nor GFP were expressed in the VZ (Fig. 2j). In *Shh:Cre:Netrin-1*$^{L/L}$ embryos, Netrin-1 mRNA was ablated from the floor plate all along the spinal cord and hindbrain at E9, E10, E11 and E13 (Fig. 2b, c, e, f and k). Netrin-1 protein was also eliminated from the floor plate at E9 but maintained in the VZ (Fig. 2g,h). Netrin-1 was not detected in E9 *Netrin-1*$^{\Delta/\Delta}$ embryos (Fig. 2i). Therefore, in *Shh:Cre;Netrin-1*$^{L/L}$ embryos, netrin-1 ablation well precedes midline crossing. The absence of netrin-1 from *Shh:Cre;Netrin-1*$^{L/L}$ floor plate was confirmed at E10-E13 (Fig. 2k, l, m and Extended Data Fig. 2a-d). Western blot analysis of floor plate extracts confirmed that netrin-1 is undetectable in *Netrin-1*$^{\Delta/\Delta}$ embryos and almost completely absent in *Shh:Cre:Netrin-1*$^{L/L}$ embryos compared to controls (Extended Data Fig. 2h, i. For gel source data see Supplementary figure 1). However, netrin-1 was still present in commissural axons, VZ and neural progenitor processes (Fig. 2l-n and Extended Data Fig. 2f, g). To determine if the absence of floor-plate netrin-1 perturbed midline crossing, we visualized commissural axons in *Shh:Cre:Netrin-1*$^{L/L}$ embryos with immunostaining for Neurofilament, Robo3, Dcc and Robo1 receptors. Robo3 is expressed by precrossing axons11, Dcc before and after crossing11, and Robo1 after crossing11. As previously described, the number of axons crossing the midline was severely reduced in the hindbrain and spinal cord in E11 and E13 *Netrin-1*$^{\beta geo/\beta geo}$ embryos compared to controls (*Shh:Cre;Netrin-1*$^{L/+}$; *Netrin-1*$^{\beta geo/+}$ or wild type; Fig. 3a, b and Extended Data Fig. 3a, b). This was confirmed by the parallel reduction in Robo1 staining. As described 8,9 , this phenotype was exacerbated in *Netrin-1*$^{\Delta/\Delta}$ embryos in which midline crossing was almost completely abolished (Fig. 3c and Extended Data Fig. 3c). Remarkably, midline crossing was not perturbed in E10-E13 *Shh:Cre;Netrin-1*$^{L/L}$ embryos, neither in the hindbrain, nor at any levels of the spinal cord (Fig. 3d and Extended Data Fig. 3d, e and data not shown). At E12, 1,1'-dioctadecyl-3,3,3',3'-tetramethylindocarbocyanine (DiI) injection in open-book hindbrains and spinal cords showed that commissural axons cross the midline and turn longitudinally in wild type and *Shh:Cre;Netrin-1*$^{L/L}$; embryos, whereas crossing is severely

perturbed in *Netrin-1*$^{ßgeo/ßgeo}$ and *Netrin-1*$^{Δ/Δ}$ embryos (Fig. 3 and not shown). Therefore, floor plate-derived netrin-1 is not required for commissural axon guidance to the floor plate.

To confirm this result, we crossed *Netrin-1*$^{L/L}$ mice to lines expressing Cre in the hindbrain. In *Foxg1:Cre;Netrin-1*$^{L/L}$ embryos, *netrin-1* mRNA is undetectable in the hindbrain VZ, but highly expressed in the floor plate (Fig. 4a, b). Accordingly, netrin-1 protein is almost absent from commissural axons and pial surface of E11 and E13 *Foxg1:Cre;Netrin-1*$^{L/L}$ hindbrains (Fig. 4a, b and Extended Data Fig. 4a, b). Netrin-1 immunoreactivity in floor plate and its vicinity, suggests that netrin does not diffuse far from it. A *Rosa*^{Tom} reporter line confirmed that *Foxg1:Cre* drives Cre expression in most of the hindbrain but only a few floor plate cells (Extended Data Fig. 4c). At E13, hindbrain commissures are strongly reduced in *Foxg1:Cre;Netrin-1*$^{L/L}$ embryos, phenocopying *Netrin-1* null embryos (Fig. 4c and Extended Data Fig. 4g and data not shown). DiI tracing of hindbrain commissural axons confirms the absence of crossing at E13 (Fig. 4c). Since VZ-netrin-1 persisted in *Foxg1:Cre;Netrin-1*$^{L/L}$ spinal cord, we could not determine if the VZ is also the netrin-1 source for spinal cord commissural axons (Extended Data Fig. 4d, e). We next studied the development of inferior olivary nucleus (ION) neurons, whose migration from the dorsal hindbrain to the floor plate is perturbed in *Netrin-1*$^{ßgeo/ßgeo}$ embryos20 (see also Fig. 1i). At E13, Foxp2+ migrating ION neurons have started to reach the floor plate in wild type mice21 (Fig. 4d). By contrast, in *Netrin-1*$^{ßgeo/ßgeo}$ (Extended Data Fig. 4f) and *Netrin-1*$^{Δ/Δ}$ embryos (Fig. 4d) most ION neurons either fail to migrate ventrally or migrate inside the hindbrain (Figs 4d and 1i). Similar defects occurred in *Foxg1:Cre;Netrin-1*$^{L/L}$ embryos but the ION migrated normally in *Shh:Cre;Netrin-1*$^{L/L}$ embryos (Fig. 4d). The role of VZ-derived netrin-1 was further investigated in E11 *Nestin:Cre;Netrin-1*$^{L/L}$ embryos22, which lack netrin-1 mRNA in VZ but not floor plate (Fig. 4e). In this mutant, a severe reduction of midline crossing was observed (Fig. 4e) an IO neuron migration was abnormal (Fig. 4e).

Netrin-1 was initially proposed as a diffusible cue, but sequence similarities with laminins and X-ray structural analyses have strengthened the view that netrin-1 is an extracellular matrix protein impacting cell adhesion4,23. This questioned the ability of netrin-1 to simply act as a soluble cue. Accordingly, studies in Drosophila netrin-1 mutants showed that the expression of a membrane-tethered netrin-1 in midline glia rescues midline crossing24. Likewise, in the Drosophila visual system, Netrin-1/Dcc interaction promotes attachment to target cells rather than chemoattraction25. In the mouse, netrin-1 attachment to a substrate is required for commissural axon extension26. We show here that during their ipsilateral extension, commissural axons respond to netrin-1 produced dorsally by neural progenitors in the hindbrain and spinal cord and that floor-plate netrin-1 is not essential. The presence of netrin-1 in dorsal spinal cord extracts14 most likely reflects its local production by neural progenitors rather than its diffusion from the floor plate. We propose that netrin-1 promotes growth cone attachment and haptotaxis, anchoring pioneer commissural axons close to the pial surface (Extended Data Fig. 4h).

Our results suggest that long-range attraction by gradient of chemoattractants is not a major guidance mechanism for commissural axons, as previously proposed 27. The role of floor plate netrin-1 is still unclear as *Shh:Cre;Netrin1*$^{L/L}$ mice are viable without any obvious behavioral defects. By contrast, *Foxg1:Cre;Netrin1*$^{L/L}$ and *Nestin:Cre;Netrin-1*$^{L/L}$ mutants

die at birth. Yet, in the spinal cord, floor plate- and VZ-derived netrin-1 might act redundantly. In the light of our results it will be important to consider floor-plate independent cellular mechanisms for the ipsilateral guidance of commissural axons.

Methods

Mouse strains and genotyping

Netrin-1$^{\beta geo}$ 7 and *DCC* 18 knockout lines were previously described and genotyped by PCR. The Netrin-1 conditional knockout was created (Genoway, Lyon, France) by inserting two *Loxp* sites flanking the coding sequences containing both the principal ATG (Based on netrin-1 cDNA sequence NM_008744) and the cryptic ATG (Based on netrin-1 cDNA: BC141294) and the alternative promoter described in intron 328.

The targeting vector was constructed as follows: three fragments of 2.1kb, 3.4kb and 4.6kb (respectively, the 5', floxed and 3' arms) were amplified by PCR using 129Sv/Pas ES DNA as a template and sequentially subcloned into the **pCR4-TOPO** vector (Invitrogen). These fragments were used for the construction of the targeting vector in which a FRT-flanked Neomycin cassette was inserted in 5' of the *Loxp*-flanked region. The linearized construct was electroporated into 129Sv/Pas mouse embryonic stem (ES) cells. After selection, targeted clones were identified by PCR using external primers and further confirmed by Southern blot analysis both with a neo and a 5' external probe. The positive ES cell clones were injected into C57BL/6J blastocysts and gave rise to male chimeras with a significant ES cell contribution. Breeding was established with C57BL/6 mice expressing the Flp-recombinase, to produce the heterozygous Netrin-1 conditional knockout line devoid of the Neomycin cassette. To generate a null-allele of netrin-1, *Netrin-1*$^{L/L}$ mice were crossed to *Krox20:Cre* mice which express Cre recombinase in the male and female germline after sexual maturity29. To ablate netrin-1 expression in the floor plate we used the *Shh:Cre* line30 (Jackson laboratories). In this line, the eGFP reporter was also inserted in the *Shh* locus. Last, we crossed *Netrin-1*$^{L/L}$ mice to *Foxg1:Cre* mice31 and *Nestin:Cre* mice22 (Jackson laboratories). The Ai9 *Rosa*^{tdTomato} reporter line (*Rosa*^{Tom}; Jackson Laboratories) was used to monitor Cre expression. Developing inferior olivary neurons were visualized by crossing the *Rosa*^{Tom} line with the *Ptf1aCre*^{ERT2} line15. They were also further crossed to *Netrin-1*$^{\beta geo}$ mice. All mice are kept in C57BL/6 background. The day of the vaginal plug was counted as embryonic day 0.5 (E0.5). Mice were anesthetized with Ketamine (100mg/ml) and Xylazine (10mg/ml). All animal procedures were carried out in accordance to institutional guidelines and approved by the UPMC University ethic committee (Charles Darwin). Embryos of either sex were used.

Tamoxifen injection

Ptf1aCre^{ERT2};Rosa^{Tom} pregnant mice were intraperitoneally injected at E10 with 1mg of tamoxifen (Sigma, T-5648) dissolved in corn oil (Sigma, C-8267). The embryos were collected at E11.

EdU labeling

Pregnant females were injected i.p. with EdU(1mg/10g) and sacrificed three hours later.

Europe PMC Funders Author Manuscripts

The proliferating cells were visualized after immunohistochemistry using the Alexa Fluor 647 Click-iT EdU Imaging Kit (Invitrogen).

In situ hybridization

Antisense riboprobes were labeled with digoxigenin-11-d-UTP (Roche Diagnostics, Indianapolis, IN) as described elsewhere12, by *in vitro* transcription of cDNA encoding mouse *netrin-1* 7 or mouse *netrin-1 exon 3*.

DiI tracing

4%PFA-fixed E12-E13 hindbrains in an open book configuration were injected using a glass micropipette with DiI crystals or small drops of DiI (Invitrogen) diluted in Dymethyl sulfoxyde (DMSO, Sigma). Samples were kept for 24hours at 37°C in 4%PFA.

Immunohistochemistry

Embryos were fixed by immersion in 4% paraformaldehyde in 0.12 M phosphate buffer, pH 7.4 (PFA) over night at 4°C. Samples were cryoprotected in a solution of 10% sucrose in 0.12M phosphate buffer (pH7.2), frozen in isopentane at 50°C and then cut at 20μm with a cryostat (Leica). Immunohistochemistry was performed on cryostat sections after blocking in 0.2% gelatin in PBS containing 0.5% Triton-X100 (Sigma). Sections were then incubated O/N with the following primary antibodies: goat anti-human Robo3 (1:250, R&D Systems AF3076), goat anti-Dcc (1:500, Santa Cruz sc-6535), goat anti-Robo1 (1:500, R&D Systems AF1749), rat anti-mouse Netrin-1 (1:500, R&D Systems MAB1109), mouse anti-Nestin-Alexa488 (1:1000, Abcam ab197495), mouse anti Neurofilament (1:300, DSHB 2H3), goat anti-Foxp2 (1:1000, Santa Cruz sc-21069), rabbit anti-Foxp2 (1:1000, Abcam AB16046), rabbit anti-Sox2 (1:500, Abcam ab97959), rabbit anti-βgal (1:500, Cappel 55976), goat anti-human Alcam (1:500, R&D Systems AF656), rabbit anti-GFP (1:800, Life Technologies A11122), rabbit anti-Dsred (1:500, Clontech 632496) followed by 2 hours incubation in species-specific secondary antibodies directly conjugated to fluorophores (Cy-5, Cy-3, Alexa-Fluor 647 from Jackson ImmunoResearch, or from Invitrogen). For netrin-1 immunostaining, an antibody retrieval treatment was performed on the sections before to process them for immunochemistry. The sections were boiled in citrate buffer (pH 6) during 9 minutes. Sections were counterstained with DAPI (1:1000,Sigma). In the case of netrin-1 immunostaining on non-permeabilized tissue, the Triton was removed from all the steps. Slides were scanned with a Nanozoomer (Hamamatsu) and laser scanning confocal microscope (FV1000, Olympus). Brightness and contrast were adjusted using Adobe Photoshop.

Whole-mount labeling and 3DISCO clearing

Whole-mount immunostaining and 3DISCO optical clearing procedure has been described previously32. 3D imaging was performed with an ultramicroscope using Inspector Pro software (LaVision BioTec).

Europe PMC Funders Author Manuscripts

Western blotting

HEK-293T cells (from ATCC, not authenticated, tested for mycoplasma contamination with a negative result) were transfected with **pCDNA3**, pCDNA3-human NTN3, pCDNA3-human NTN1 or pCDNA3-mouse ntn1 plasmids using Fugene HD transfection reagent (Promega) according to the manufacturer's instructions. Cells were harvested and lysed 36 hr after transfection. Cells were lysed using RIPA buffer (150 mM NaCl, 50 mM Tris pH 8.0, 1% NP-40, 0.5% sodium deoxycholate, 0.1% SDS, complete protease inhibitor cocktail (Roche)) and incubated 1 hr at 4°C. Floor plates were micro-dissected from hindbrains and spinal cords from *Netrin-1*$^{L/L}$, *Shh:Cre;Netrin-1*$^{L/L}$ and *Netrin-1*$^{\Delta/\Delta}$ E11 embryos. Floor plates were lysed in RIPA buffer and incubated 20 min at 4°C. Protein content was determined by a BCA assay. 25 µg of total proteins were loaded on a 10% Mini Protean TGX precast gel (Biorad) and blotted onto a nitrocellulose membrane (Biorad). Membranes were blocked with 5% dried milk and 3% of BSA in TBS-0.1% Tween (TBS-T) for 1 hr at room temperature and incubated for 1 hr and 30 min at room temperature with primary antibodies: anti-Actin (Sigma, A5060, rabbit polyclonal, 1:1500), anti-HPRT (Abcam, ab109021, rabbit monoclonal EPR5299, 1:10000), anti-Netrin-1 (R&D Systems, MAB1109, rat monoclonal, 1:500), anti-Netrin-3 (Abcam, ab185200, rabbit polyclonal, 1:1000) and anti-Slit2 (Abcam, ab134166, rabbit monoclonal, 1:400). After three washes in TBS-T, membranes were incubated with the appropriate HRP-conjugated secondary antibody (1:5000, Jackson ImmunoResearch, Suffolk, UK). Detection was performed using Pierce ECL Western Blotting Substrate (ThermoScientific).

Data quantification and statistics

All data quantification was done by an observer blinded to the experimental conditions. We did not perform randomization into groups. Data were presented as mean values ± standard error of the mean. Statistical significance was calculated using one-sided unpaired tests for non-parametric tendencies (Kruskal-Wallis and Mann-Whitney). For western blot, at least 3 independent cases were quantified from independent experiments using densitometric analysis (Image J) by normalizing phospho-signals to total protein levels. The control cases were normalized to 1 and for the mutants, data were presented as mean values ± standard error of the mean (0.1133 ± 0.05 for *Shh:Cre;* 1 for *Netrin-1*$^{L/L}$ and 0 for the *Netrin-1*$^{\Delta/\Delta}$). Differences were considered significant (*) when $P<0.05$. Statistical test data were as follows; Extended Data 2**i**, *Netrin-1*$^{L/L}$ to *Shh:Cre; Netrin-1*$^{L/L}$ or *Netrin-1*$^{\Delta/\Delta}$ Mann-Whitney test, $P<0.05$ ($P=0.0022$ for both). The thickness of hindbrain commissural bundles was quantified for each embryo on 9 coronal sections. The sections were representative of 3 different hindbrain antero-posterior levels (3 sections for each level). To minimize the developmental variations, mutant embryos and littermate controls were compared (except for *Netrin-1*$^{\Delta/\Delta}$ embryos which were compared with wild type embryos). The ratio of the commissural axon bundle size was normalized to controls. Six embryos of each genotype were quantified, from at least two different litters. Data were presented as mean values ± standard error of the mean. For the Wt (Dcc 0.994 ± 0.052; Robo3 1 ± 0.061; Neurofilament 1 ± 0.048), *Netrin-1*$^{ßgeo/ßgeo}$ (Dcc 0.416 ± 0.013; Robo3 0.402 ± 0.007; Neurofilament 0.416 ± 0.01), *Netrin-1*$^{\Delta/\Delta}$ (Dcc 0.091 ± 0.008; Robo3 0.061 ± 0.008; Neurofilament 0.104 ± 0.007) *Shh:Cre;Netrin-1*$^{L/L}$ (Dcc 1.051 ± 0.011; Robo3 1.084 ± 0.028; Neurofilament

1.063 ± 0.019) and *Foxg1:Cre;Netrin-1*$^{L/L}$ (Dcc 0.411 ± 0.053; Robo3 0.369 ± 0.056; Neurofilament 0.416 ± 0.050).

Differences were considered significant (*) when P<0.05. Statistical test data were as follows; Extended Data Fig. 4g, Dcc, Robo3 and Neurofilament Kruskal-Wallis, P<0.05. Extended Data Fig. 4g, comparison between wild type and the different conditions for Dcc, Robo3 and Neurofilament, Mann-Whitney, P<0.05. Except the comparison between wild type and *Shh:Cre;Netrin-1*$^{L/L}$ where, Dcc Mann-Whitney, P=0.0649, Robo3 Mann-whitney, P=0.1797, Neurofilament Mann-whitney, P=0.0649. Statistical analyses of the mean and variance were performed with Prism 7 (GraphPad Software).

Europe PMC Funders Author Manuscripts

Europe PMC Funders Author Manuscripts

Extended Data

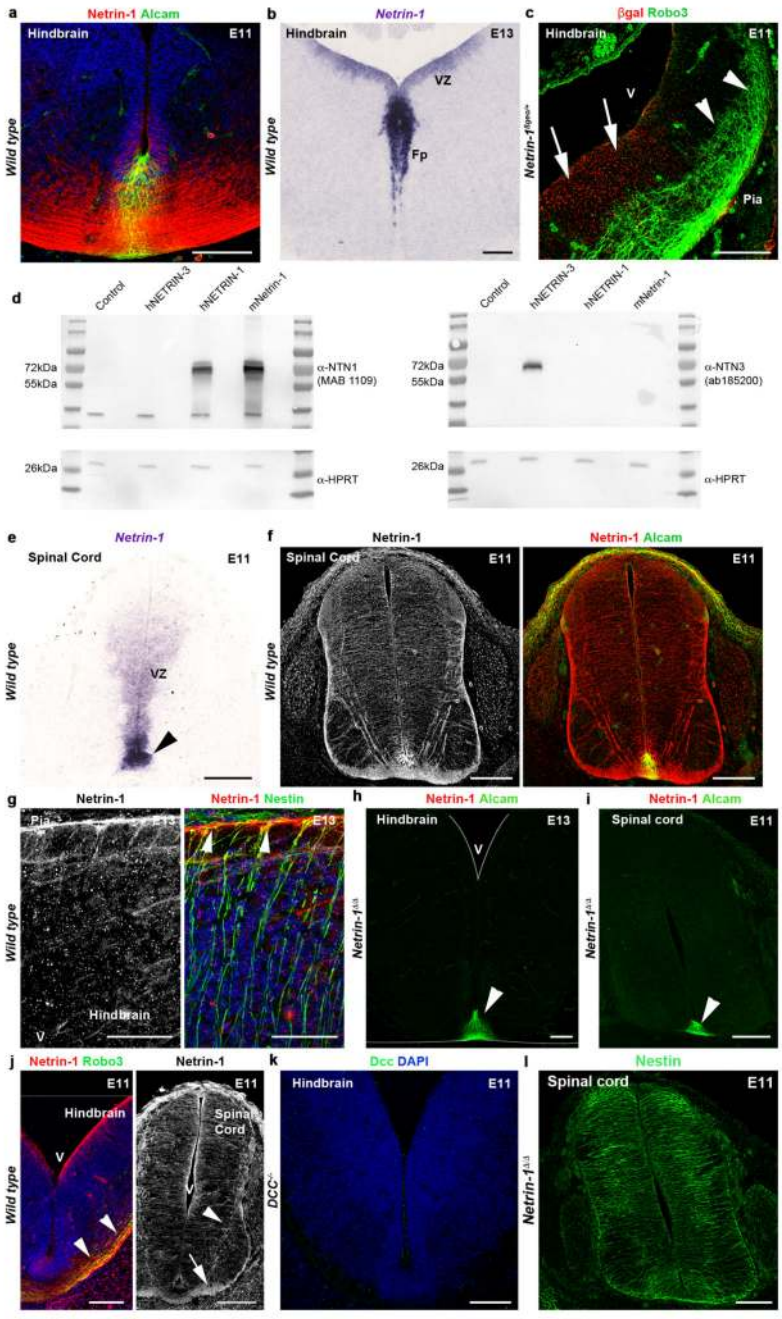

Extended Data Figure 1. Netrin-1 distribution in Hindbrain and Spinal Cord

Coronal cryostat sections of the hindbrain and spinal cord (brachial level) of E11 and E13 embryos.

a, At E11, the floor plate (Alcam+ positive cells in green) but also commissural axons are immunoreactive for netrin-1 (n=6). **b,** At E13 *netrin-1 mRNA* is still expressed in the floor plate (Fp) and VZ of the basal plate (n=6). **c**, In a E11 *Netrin1*$^{\beta geo/+}$, Robo3+ commissural

Europe PMC Funders Author Manuscripts

neurons in the dorsal hindbrain (arrowheads) are not immunoreactive for ßgal unlike the basal plate neuroepithelium (arrows; n=6). **d**, Western blot analysis of HEK-293T cells overexpressing hNETRIN-3, hNETRIN-1 or mNetrin-1 proteins (n=3). Left, the monoclonal anti-NTN1 antibody (MAB1109) specifically recognizes Netrin-1 proteins (human and mouse) and not Netrin-3. Right, Netrin-3 is specifically recognized by the polyclonal anti-NTN3 antibody (ab185200) unlike Netrin-1. **e**, At E11, netrin-1 is expressed in the spinal cord by floor plate (arrowhead) and VZ progenitors (n=6). **f**, The floor plate (Alcam+), commissural axons, radial processes of neural progenitors and basal lamina are immunoreactive for netrin-1 (n=6). **g**, At E13 (n=7), netrin-1 is still highly distributed in Nestin+ radial processes of neural progenitors and at the pial surface. **h**,**i** Netrin-1 protein is absent from the hindbrain of *Netrin-1*$^{\Delta/\Delta}$ at E13 (**h**) and the spinal cord at E11 (**i**) (n=6 for each). Floor plate cells (arrowhead) still express Alcam (green). **j**, Netrin-1 immunostaining without permeabilization at E11. Commissural axons are still labeled (arrowheads) including post-crossing ones (arrow). Commissural axons are also stained with anti-Robo3 on the left panel. Ventricle (V). **k,** Shows the absence of Dcc-immunoreactivity on a hindbrain section from a *DCC*$^{-/-}$ E11 embryo (DAPI counterstaining, n=6). **l**, Neural progenitors radial processes are present in *Netrin-1*$^{\Delta/\Delta}$ embryos (n=6). Scale bars, 100 μm except in **g**, 50 μm.

Europe PMC Funders Author Manuscripts

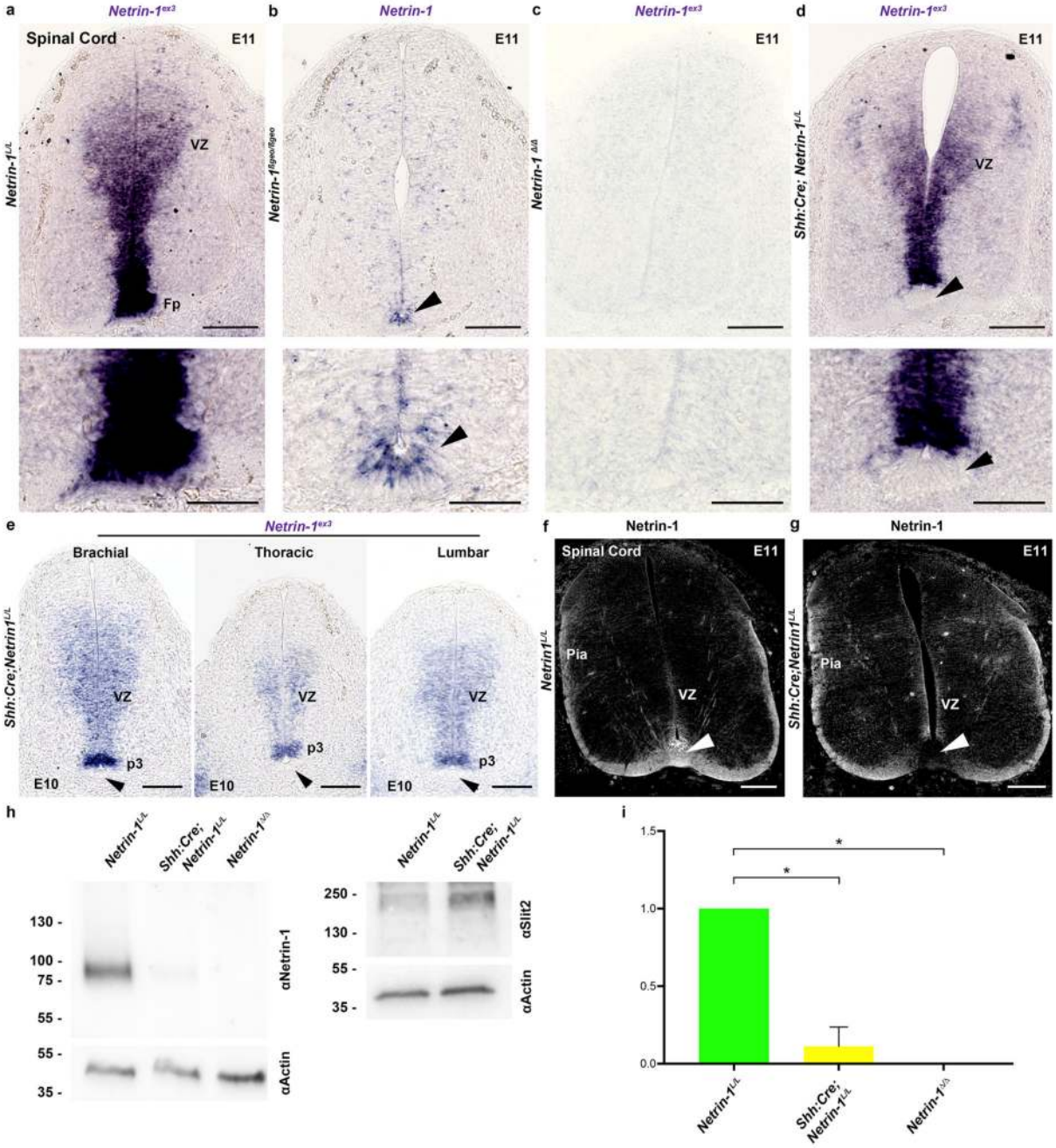

Extended Data Figure 2. Floor plate-specific deletion of netrin-1 in *Shh:Cre;Netrin1^{lox}* mutants.

Coronal cryostat sections of the hindbrain and spinal cord of E10 and E11 embryos. **a-d,** *In situ* hybridization for *netrin-1* on E11 spinal cord (brachial level). In *Netrin-1$^{L/L}$* embryo (**a**) *netrin-1* mRNA is highly expressed in floor plate (Fp) and ventricular zone (VZ) (n=6). A weak *netrin-1* expression is still detected in the floor plate (arrowhead) of a *Netrin1$^{ßgeo/ßgeo}$* hypomorph (**b**) (n=5), whereas no signal is seen in a *Netrin-1$^{Δ/Δ}$* (**c**) embryo (n=6). In *Shh:Cre;Netrin1$^{L/L}$* embryo (**d**), netrin-1 mRNA is not expressed in the floor plate (arrowhead) but still present in the VZ (n=6). **e,** E10 *Shh:Cre;Netrin$^{L/L}$* spinal cord sections

Europe PMC Funders Author Manuscripts

at brachial, thoracic and lumbar levels. At all levels, *Netrin-1* is found in the VZ, with the highest levels in the p3 progenitor domain, but is absent from the floor plate (arrowheads, n=6). **f,g,** In *Netrin-1*$^{L/L}$ (**f**) commissural axons, basal lamina (Pia) and floor plate (arrowhead in **f**) are immunoreactive for netrin-1. By contrast, the floor plate is not labeled in *Shh:Cre;Netrin1*$^{L/L}$ embryos (arrowhead in **g**) whereas netrin-1 remains expressed along neural progenitor processes and basal lamina (Pia; n=6/6). **h**, Western blot with Netrin-1 antibody on floor plate extracts from *Netrin-1*$^{L/L}$, *Shh:Cre;Netrin*$^{L/L}$ and *Netrin-1*$^{\Delta/\Delta}$ E11 embryo hindbrain and spinal cord (at least 3 cases for each from 3 independent experiments). Netrin-1 is undetectable in *Netrin-1*$^{\Delta/\Delta}$ and reduced of 90% in *Shh:Cre;Netrin*$^{L/L}$. **i,** Western blot quantification. Wild type values were normalized to 1 and mutant values were compared to it using a non-parametric Mann-Whitney test. Mutant values are represented as the mean ± SEM (*P<0.05). Scale bars, 100 μm, except on a, b, c and d higher magnifications, 50 μm.

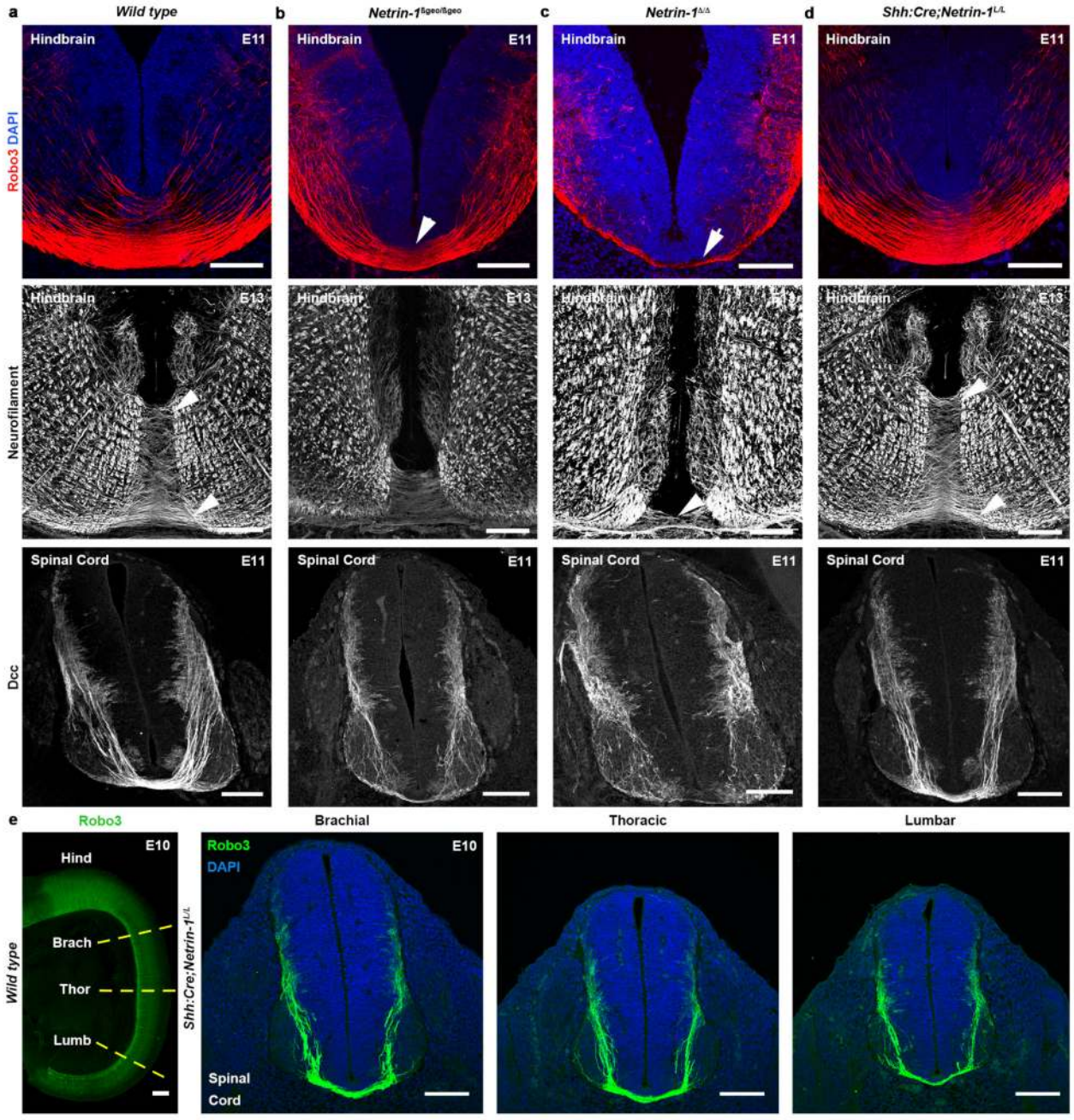

Extended Data Figure 3. Floor plate-derived netrin-1 is not necessary for the midline crossing in hindbrain and spinal cord.

Coronal cryostat sections of the hindbrain and spinal cord (brachial level) of E10, E11 and E13 embryos . **a-d**, E11 and E13 hindbrain sections (upper and middle panels) and E11 spinal cord sections (lower panels). In wild type (**a**) Robo3+ and Dcc+ commissural axons cross the floor plate (n=6). Midline crossing is reduced in *Netrin1*$^{ßgeo/ßgeo}$ hypomorphs (**b**; arrowheads; n=3) and almost absent in *Netrin-1*$^{Δ/Δ}$ embryos (**c**; n=6). By contrast, no midline crossing defects are present in *Shh:Cre;Netrin1*$^{L/L}$ embryos (**d**) (n=9). **e,** Coronal

sections at 3 rostro-caudal levels of the spinal cord of an E10 *Shh:Cre;Netrin-1$^{L/L}$* embryo labeled with anti-Robo3. Commissural axons cross the floor plate at all levels. The dashed lines on the left panel shows the level of the sections. Abbreviations: Brach: brachial; Hind, hindbrain; Thor, thoracic; Lumb, lumbar. Scale bars, 100 μm, except on **e** left panel, 400 μm.

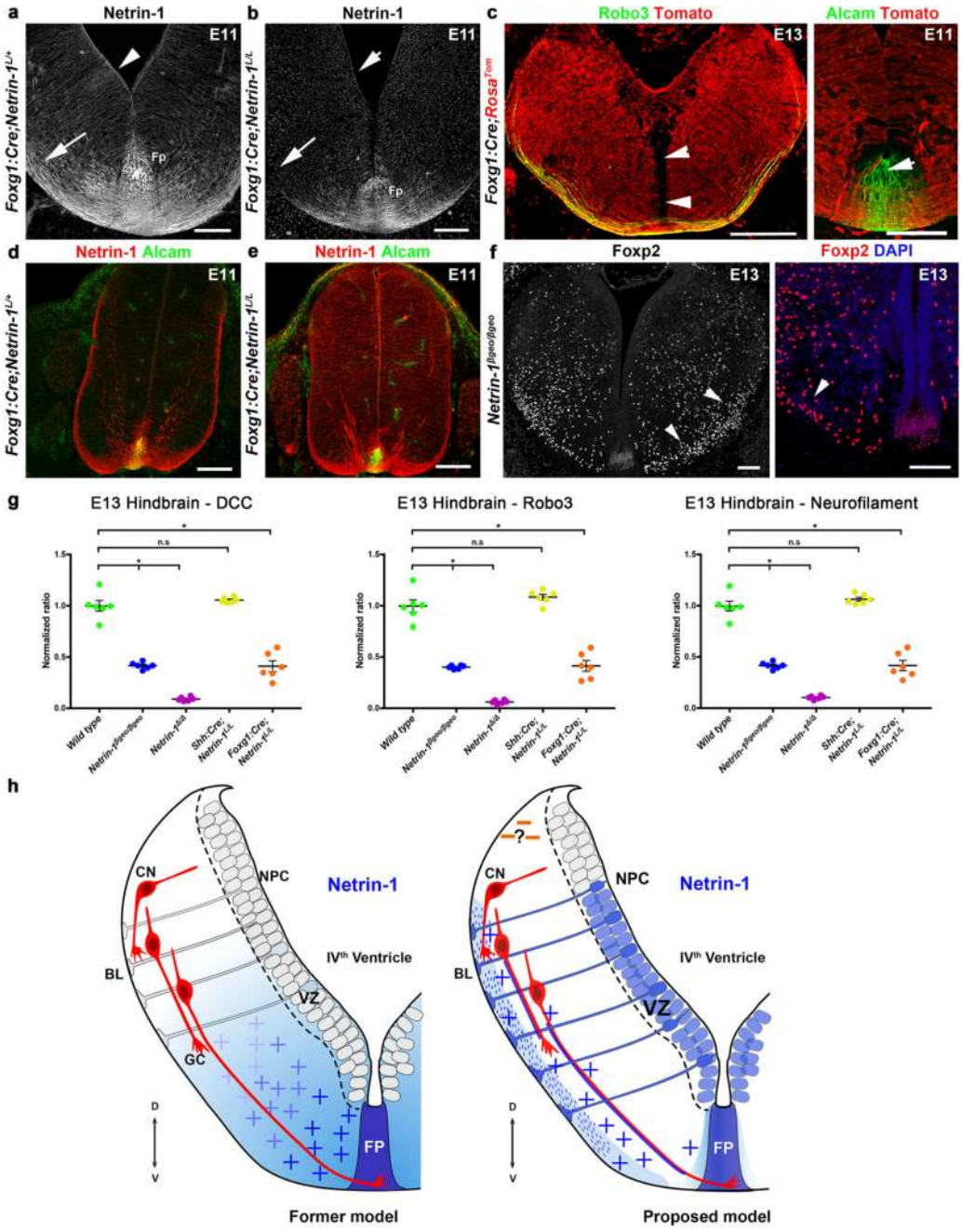

Extended Data Figure 4. Analysis of the *Foxg1:Cre ;Netrin-1^{lox}* mice.

Coronal cryostat sections of the hindbrain of E11 and E13 embryos and spinal cord (brachial level) of E11 embryos **. a-b**, In *Foxg1:Cre;Netrin-1$^{L/+}$* embryos as in wild type, netrin-1 is in

Europe PMC Funders Author Manuscripts

the hindbrain VZ (arrowhead) and commissural axons (arrow). This is not the case in *Foxg1:Cre;Netrin-1*$^{L/L}$ mutant. The floor plate is still labelled (Fp). Note that netrin-1 is present in the vicinity of the Fp (n=6). **c**, *Foxg1:Cre* drives Cre expression in E13 (left) and E11 (right) hindbrain cells (Tomato+ cells in red) but not in the floor plate (arrowheads; n=3/3). A few Alcam+ floor plate cells are Tomato+. **d, e,** Netrin-1 distribution is similar in the spinal cord of *Foxg1:Cre;Netrin-1*$^{L/+}$ **(d)** and *Foxg1:Cre;Netrin-1*$^{L/L}$ (**e**) embryos (n=5). **f**, In *Netrin1*$^{ßgeo/ßgeo}$, Foxp2+ olivary neurons fail to migrate (arrowheads) ventrally and only few of them are able to reach to the floor plate (arrowheads; n=6). **g**, Quantification of the size of hindbrain commissures in the different mutants compared to controls. Six embryos of each genotype and 9 sections from each were quantified. Data are normalized with the wt and are represented as the mean ± SEM (One-way Kruskal-Wallis with Mann-Whitney post-test, *P<0.05, ns, not significant). **h,** Netrin-1 guidance mechanisms of hindbrain commissural axons: past and current models. In the initial model, soluble netrin-1 secreted by floor plate (FP) forms a ventro-dorsal gradient, which attracts ventrally commissural axon (CN) growth cones (GC). In the revised model, pioneer CN axons form in a superficial region containing high levels of netrin-1 produced by neural progenitor cells (NPCs) extending from the ventricular zone (VZ) to the basal lamina (BL) at the surface of the hindbrain. CN axons might also capture Netrin-1 and establish a netrin-1-rich pathway guiding follower axons. Their ventral extension might be facilitated by chemorepellents (question mark) produced in the dorsal hindbrain. Scale bars, 100µm.

Supplementary Material

Refer to Web version on PubMed Central for supplementary material.

Acknowledgements

We thank Dr Marc Tessier-Lavigne for providing the *DCC* and *Netrin-1* knockout Dr Christopher Wright for the *Ptf1a:Cre*^{ERT2} line and Dr Patrick Charnay for the *Krox20:Cre* line. We also thank Alex Kolodkin and Robin Vigouroux for critical reading of the manuscript and Stéphane Fouquet of the Vision Institute imaging facility for its technical support. This work was supported by grants from the Agence Nationale de la Recherche (ANR-14-CE13-0004-01) (AC). It was performed in the frame of the LABEX LIFESENSES (reference ANR-10-LABX-65) supported by French state funds managed by the ANR within the Investissements d'Avenir programme under reference ANR-11-IDEX-0004-02 (AC). This work was also supported by grants from INCA, ERC, ANR and Fondation Bettencourt (PM). C.D was recipient of a PhD fellowship from the Fondation pour la recherche médicale.

References

1. Serafini T, et al. The netrins define a family of axon outgrowth-promoting proteins homologous to C. elegans UNC-6. Cell. 1994; 78:409–424. [PubMed: 8062384]
2. Ishii N, Wadsworth WG, Stern BD, Culotti JG, Hedgecock EM. UNC-6, a laminin-related protein, guides cell and pioneer axon migrations in C. elegans. Neuron. 1992; 9:873–881. [PubMed: 1329863]
3. Mitchell KJ, et al. Genetic analysis of Netrin genes in Drosophila: Netrins guide CNS commissural axons and peripheral motor axons. Neuron. 1996; 17:203–215. [PubMed: 8780645]
4. Kennedy TE, Serafini T, de la Torre J, Tessier-Lavigne M. Netrins are diffusible chemotropic factors for commissural axons in the embryonic spinal cord. Cell. 1994; 78:425–435. [PubMed: 8062385]
5. Ming GL, et al. cAMP-dependent growth cone guidance by netrin-1. Neuron. 1997; 19:1225–1235. [PubMed: 9427246]

Europe PMC Funders Author Manuscripts

6. de la Torre JR, et al. Turning of retinal growth cones in a netrin-1 gradient mediated by the netrin receptor DCC. Neuron. 1997; 19:1211–1224. [PubMed: 9427245]
7. Serafini T, et al. Netrin-1 is required for commissural axon guidance in the developing vertebrate nervous system. Cell. 1996; 87:1001–14. [PubMed: 8978605]
8. Yung, aR, Nishitani, aM, Goodrich, LV. Phenotypic analysis of mice completely lacking Netrin-1. Development. 2015; 142:3686–3691. [PubMed: 26395479]
9. Bin JMM, et al. Complete Loss of Netrin-1 Results in Embryonic Lethality and Severe Axon Guidance Defects without Increased Neural Cell Death. Cell Rep. 2015; 12:1099–106. [PubMed: 26257176]
10. Chédotal A. Development and plasticity of commissural circuits: from locomotion to brain repair. Trends Neurosci. 2014; 37:551–62. [PubMed: 25220044]
11. Sabatier C, et al. The divergent Robo family protein rig-1/Robo3 is a negative regulator of slit responsiveness required for midline crossing by commissural axons. Cell. 2004; 117:157–69. [PubMed: 15084255]
12. Marillat V, et al. The slit receptor Rig-1/Robo3 controls midline crossing by hindbrain precerebellar neurons and axons. Neuron. 2004; 43:69–79. [PubMed: 15233918]
13. Wentworth LE. The development of the cervical spinal cord of the mouse embryo. II. A Golgi analysis of sensory, commissural, and association cell differentiation. J Comp Neurol. 1984; 222:96–115. [PubMed: 6699204]
14. Kennedy TE, Wang H, Marshall W, Tessier-Lavigne M. Axon guidance by diffusible chemoattractants: a gradient of netrin protein in the developing spinal cord. J Neurosci. 2006; 26:8866–8874. [PubMed: 16928876]
15. Fleming JT, et al. The Purkinje neuron acts as a central regulator of spatially and functionally distinct cerebellar precursors. Dev Cell. 2013; 27:278–92. [PubMed: 24229643]
16. Renier N, et al. Genetic Dissection of the Function of Hindbrain Axonal Commissures. PLoS Biol. 2010; 8:e1000325. [PubMed: 20231872]
17. Hiramoto M, Hiromi Y, Giniger E, Hotta Y. The Drosophila Netrin receptor Frazzled guides axons by controlling Netrin distribution. Nature. 2000; 406:886–889. [PubMed: 10972289]
18. Fazeli A, et al. Phenotype of mice lacking functional Deleted in colorectal cancer (Dcc) gene. Nature. 1997; 386:796–804. [PubMed: 9126737]
19. Joksimovic M, et al. Wnt antagonism of Shh facilitates midbrain floor plate neurogenesis. Nat Neurosci. 2009; 12:125–31. [PubMed: 19122665]
20. Bloch-Gallego E, Ezan F, Tessier-Lavigne M, Sotelo C. Floor plate and netrin-1 are involved in the migration and survival of inferior olivary neurons. J Neurosci. 1999; 19:4407–20. [PubMed: 10341242]
21. Fujita H, Sugihara I. FoxP2 expression in the cerebellum and inferior olive: development of the transverse stripe-shaped expression pattern in the mouse cerebellar cortex. J Comp Neurol. 2012; 520:656–77. [PubMed: 21935935]
22. Tronche F, et al. Disruption of the glucocorticoid receptor gene in the nervous system results in reduced anxiety. Nat Genet. 1999; 23:99–103. [PubMed: 10471508]
23. Grandin M, et al. Structural Decoding of the Netrin-1/UNC5 Interaction and its Therapeutical Implications in Cancers. Cancer Cell. 2016; 29:173–185. [PubMed: 26859457]
24. Brankatschk M, Dickson BJ. Netrins guide Drosophila commissural axons at short range. Nat Neurosci. 2006; 9:188–94. [PubMed: 16429137]
25. Akin O, Zipursky SL. Frazzled promotes growth cone attachment at the source of a Netrin gradient in the Drosophila visual system. Elife. 2016; 5
26. Moore SW, Biais N, Sheetz MP. Traction on immobilized netrin-1 is sufficient to reorient axons. Science. 2009; 325:166. [PubMed: 19589994]
27. Matise M, Lustig M, Sakurai T, Grumet M, Joyner A. Ventral midline cells are required for the local control of commissural axon guidance in the mouse spinal cord. Development. 1999; 126:3649–3659. [PubMed: 10409510]
28. Delloye-Bourgeois C, et al. Nucleolar Localization of a Netrin-1 Isoform Enhances Tumor Cell Proliferation. Sci Signal. 2012; 5:ra57–ra57. [PubMed: 22871610]

29. Voiculescu O, Charnay P, Schneider-Maunoury S. Expression pattern of a Krox-20/Cre knock-in allele in the developing hindbrain, bones, and peripheral nervous system. genesis. 2000; 26:123–6. [PubMed: 10686605]

30. Harfe BD, et al. Evidence for an expansion-based temporal Shh gradient in specifying vertebrate digit identities. Cell. 2004; 118:517–528. [PubMed: 15315763]

31. Hébert JM, Mcconnell SK. Targeting of cre to the Foxg1 (BF-1) locus mediates loxP recombination in the telencephalon and other developing head structures. Dev Biol. 2000; 222:296–306. [PubMed: 10837119]

32. Belle M, et al. A Simple Method for 3D Analysis of Immunolabeled Axonal Tracts in a Transparent Nervous System. Cell Rep. 2014; 9:1191–1201. [PubMed: 25456121]

Europe PMC Funders Author Manuscripts

Europe PMC Funders Author Manuscripts

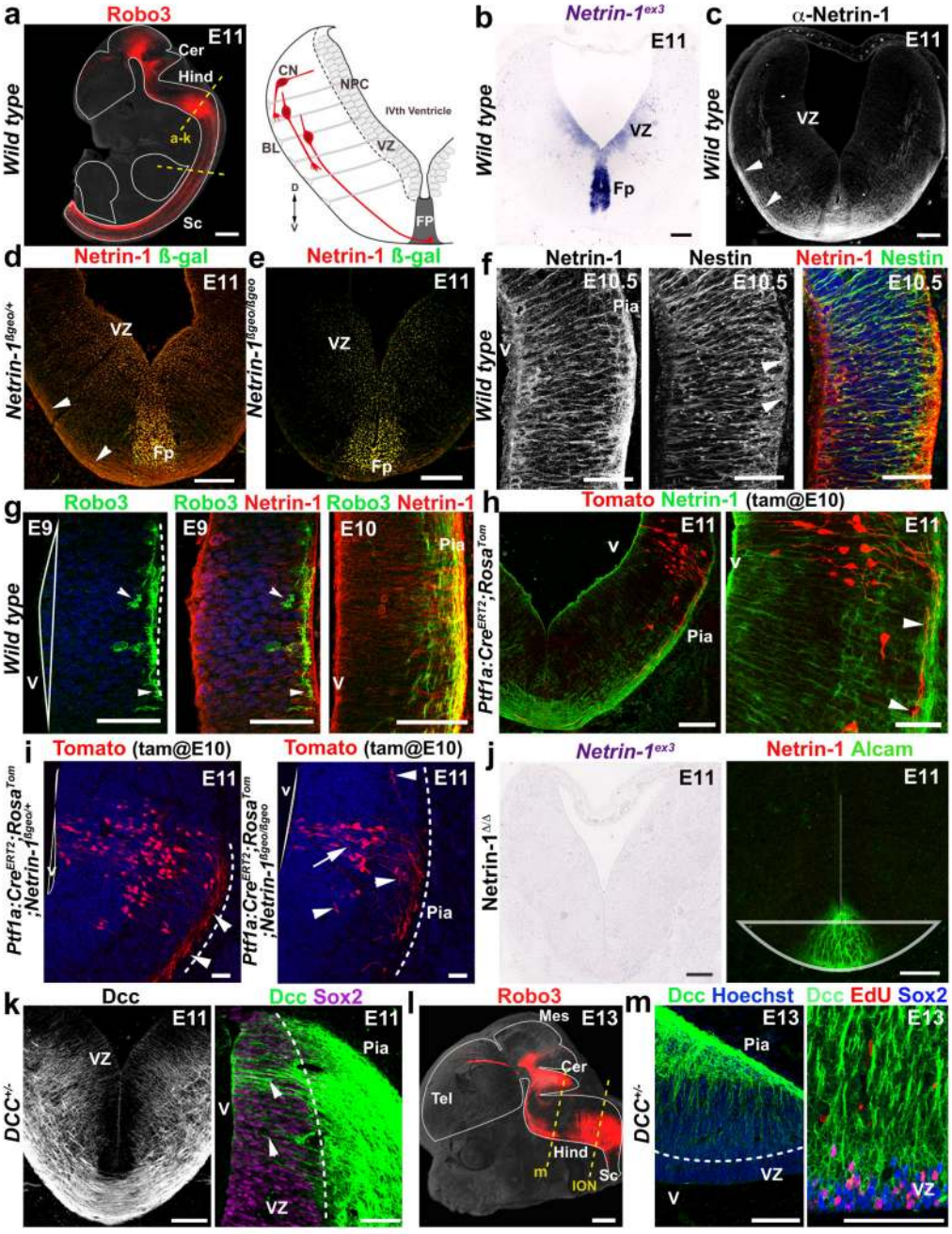

Figure 1. Netrin-1 is expressed by ventricular zone neural progenitors.

a Robo3+ commissural axons (left) and hindbrain schematic (right). Dashed lines show section levels. **b,** In wild type, *netrin-1* mRNA is in VZ and Fp (n=6). **c**, Netrin-1 protein is in Fp and commissural axons (arrowheads; n=6). **d,e,** In *Netrin-1*$^{ßgeo/+}$ (**d**) and *Netrin-1*$^{ßgeo/ßgeo}$ (**e**), the netrin-1-ß-gal protein is in the VZ and Fp (n=6 and 6). Commissural axons (arrowheads) are netrin-1+ but ßgal-. **f,** netrin-1 is detected in Nestin+ radial processes extending to the pia (arrowheads; n=6). **g**, the first Robo3+ commissural growth cones (arrowheads; n=6) extend under the pia (dotted line) in a netrin-1-rich domain.

h,i, Tomato+ inferior olivary growth cones (arrowheads) extend ventrally in a netrin-1-rich domain in *Ptf1a:Cre*^{ERT2}*;Rosa*^{Tom} and *Netrin-1*$^{\beta geo/+}$ (n=6). In *Netrin-1*$^{\beta geo/\beta geo}$ (n=6), axons (arrowheads) stall at the pial surface and some enter the VZ (arrow). **j**, Absence of *netrin-1* mRNA and protein (n=6 each) in *Netrin-1*$^{\Delta/\Delta}$ hindbrain. **k**, DCC labels hindbrain commissural axons and radial processes (arrowheads) extending from the Sox2+ VZ (n=6). **l,** Robo3+ commissural axons at E13. **m**, Sox2+/EdU+ cerebellar VZ progenitors express DCC (n=6). Abbreviations: Cerebellum (Cer); Hindbrain (Hind), spinal cord (Sc); Neural precursors (NPC), ventricular zone (VZ), basal lamina (BL); commissural neurons (CN), floor plate (Fp). Scale bars, 500 μm (a, l); 50 μm (g, h right panel, m); 100 μm (all other panels).

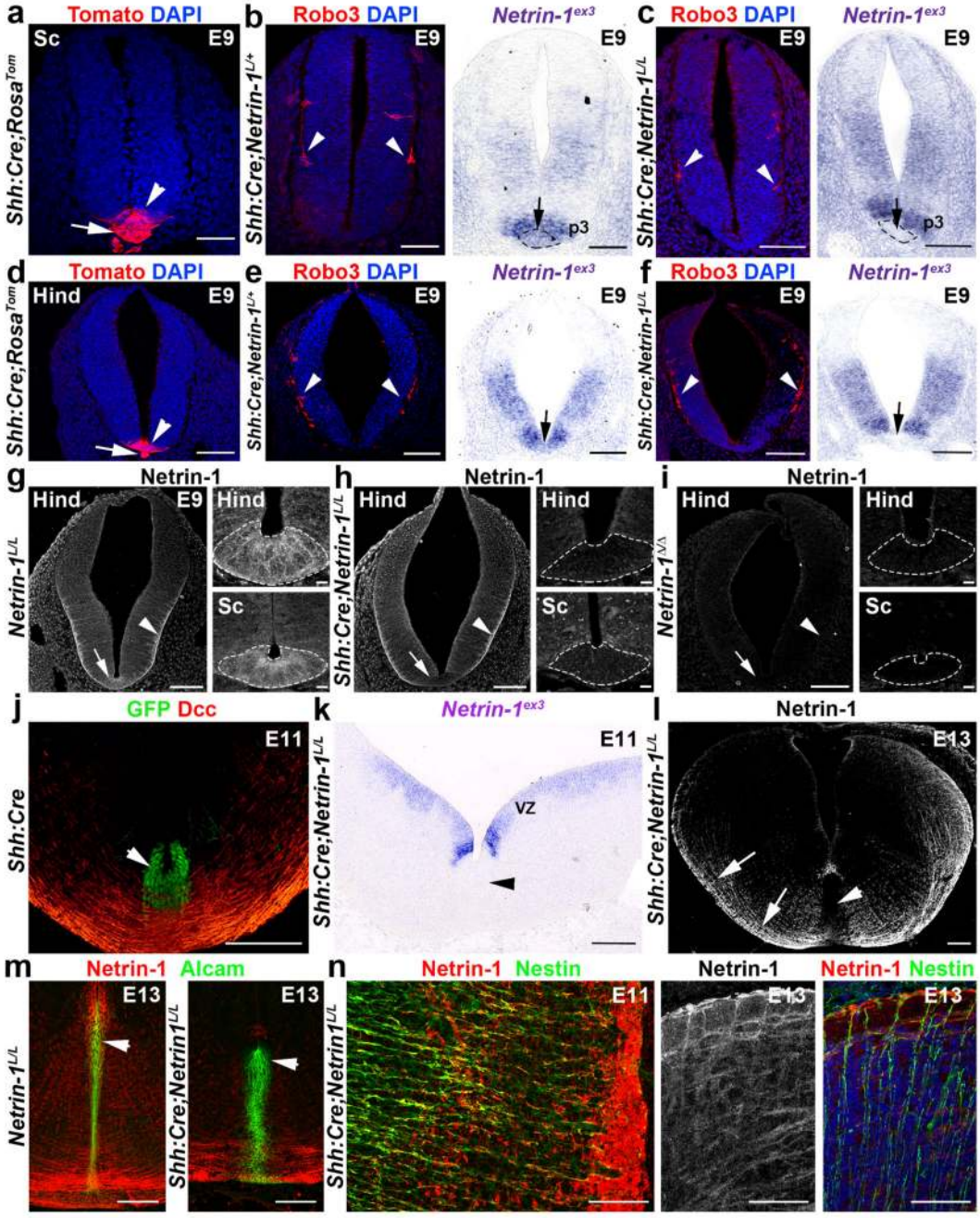

Figure 2. Floor plate-specific deletion of netrin-1 in *Shh:Cre;Netrin-1^{lox}* embryos

a-f, Tomato is expressed in the floor plate (arrowhead) and notochord (arrow) in *Shh:Cre;Rosa^{Tom}* spinal cord (**a**) and hindbrain (**d**) (n=6). Robo3+ commissural axons (arrowheads in **b, c, e and f**) have not reached the midline. *Netrin-1* mRNA is in the floor plate (short arrows) in *Shh:Cre;Netrin$^{L/+}$* but not in *Shh:Cre;Netrin$^{L/L}$*. **g-i**, Netrin-1 is in floor plate (arrow) and pial surface (arrowhead) in the wild type (**g;** n=6). In *Shh:Cre;Netrin-1$^{L/L}$* (**h**; n=6), netrin-1 is absent from floor plate (arrow and dotted lines) but present at the pial surface (arrowhead). Netrin1 is completely absent in *Netrin-1$^{Δ/Δ}$* (**i**; n=6).

Europe PMC Funders Author Manuscripts

j, In *Shh:Cre*, GFP is in floor plate (arrowhead; n=6). Commissural axons express Dcc. **k**, *Netrin-1* is absent from floor plate but maintained in VZ (n=6). **l-n,** In *Shh:Cre;Netrin-1*$^{L/L}$, floor plate (arrowheads in l) lacks Netrin-1, but not commissural axons (short arrows in **l**) and Nestin+ neural progenitors (**n**; n=6). Alcam expression is unchanged in floor plate (arrowheads in **m**; n=6). In *Shh:Cre;Netrin-1*$^{L/L}$ (**n**) Nestin+ processes still express netrin-1 (n=6).

Scale bars are 100 μm except on the higher magnifications of g, h, I where they are 10μm.

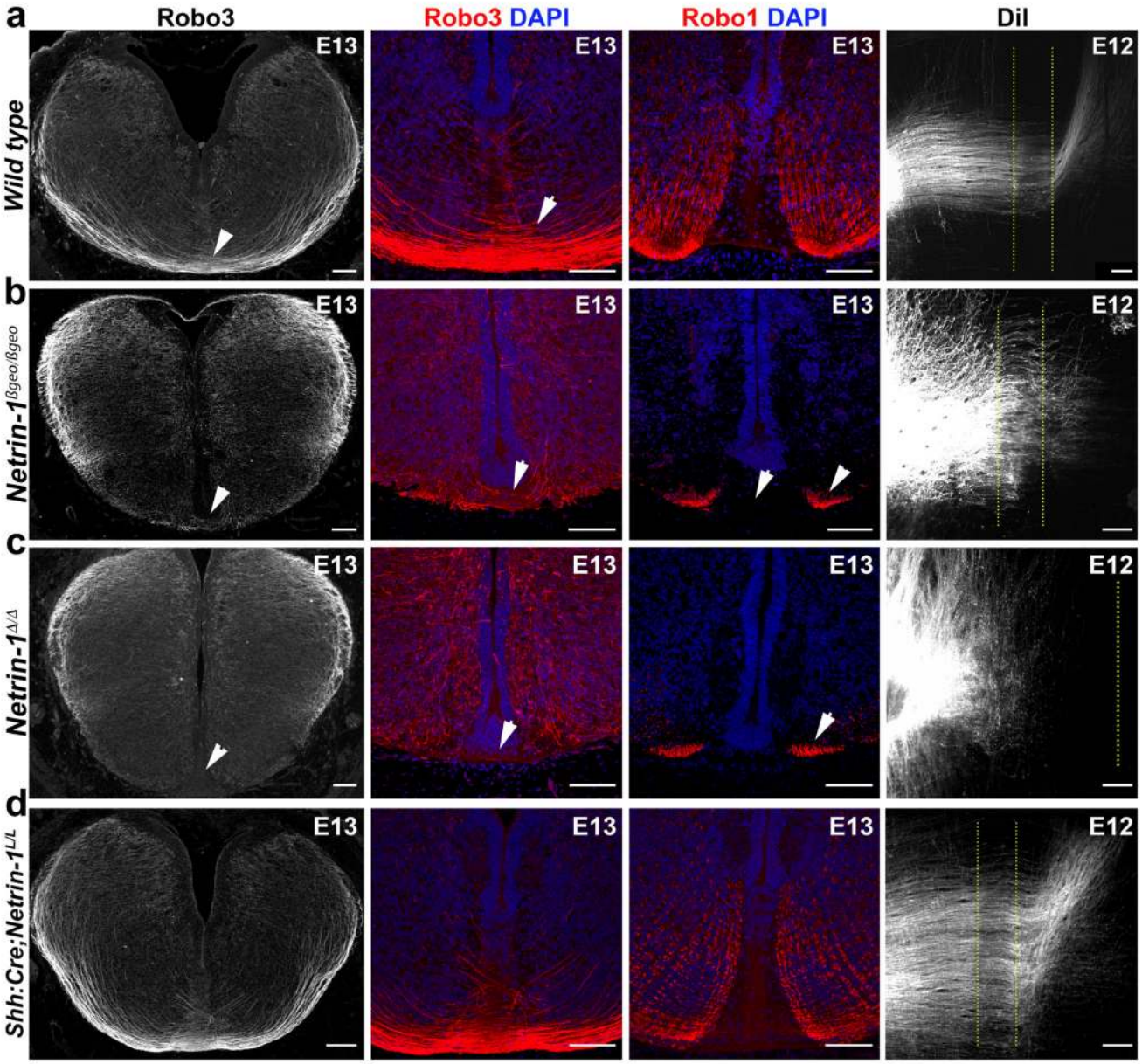

Figure 3. Commissural axons develop normally without floor plate-derived netrin-1.

Coronal sections and flat-mounts of E12 and E13 hindbrains. **a**, In wild type, Robo3+ commissural axons cross the floor plate (arrowheads) and Robo1 is on post-crossing axons (n=7). DiI-labeled commissural axons cross the midline (dotted lines) and turn longitudinally (n=5). **b**, In *Netrin-1*$^{ßgeo/ßgeo}$, midline crossing is reduced (arrowheads) and most DiI-labeled axons fail to cross (n=3). **c**, Crossing is strongly reduced in *Netrin-1*$^{Δ/Δ}$ (n=6). Robo1 is still expressed on the few crossing axons (arrowheads in **b** and **c**; n=6). **d**, Commissures look similar to control in *Shh:Cre;Netrin-1*$^{L/L}$ (n=6).

Scale bars, 100 μm.

Europe PMC Funders Author Manuscripts

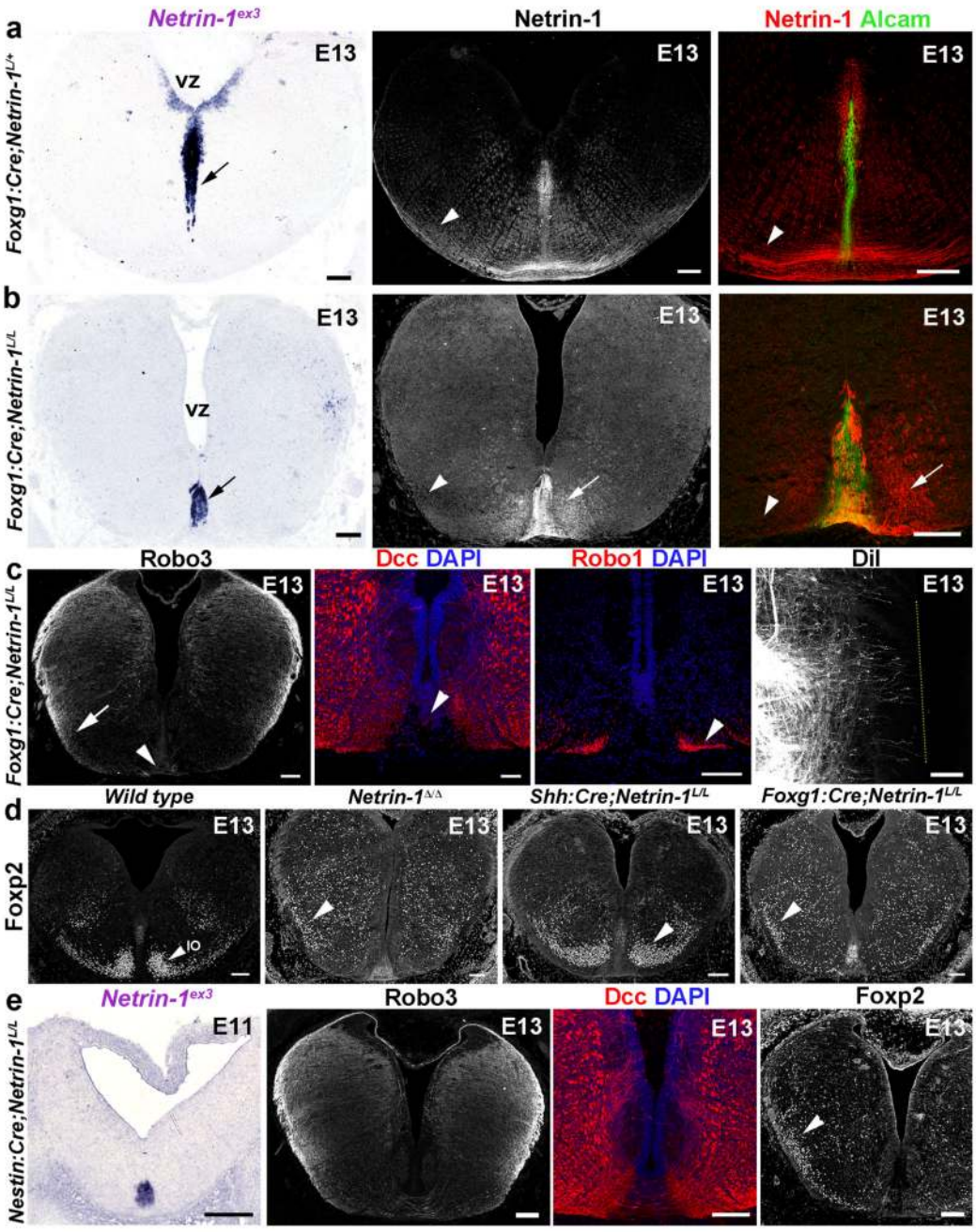

Figure 4. Ventricular zone-derived netrin-1 controls commissural axon guidance.

a, b, VZ-Netrin-1 is absent in *Foxg1:Cre;Netrin-1$^{L/L}$* and reduced on commissural axons (arrowheads). Netrin-1 is still found in floor plate (short arrows; 5/5). **c,** A few commissural axons (arrowheads; n=6) cross the midline (arrow) and DiI-labeled axons fail to cross (dotted line; n=6). **d**, in wild type Foxp2+ olivary neurons (IO) have started to reach the floor plate (arrowhead; n=7). Most IO neurons fail to migrate ventrally (arrowheads; n=6) in *Netrin-1$^{\Delta/\Delta}$* and *Foxg1:Cre;Netrin-1$^{L/L}$*, unlike in *Shh:Cre;Netrin-1$^{L/L}$* (n=7). **e**, Netrin-1 expression (n=6). Midline crossing and IO neuron migration are impaired (n=6).

Scale bars,100 μm.

Europe PMC Funders Author Manuscripts